Astron. Astrophys. 261, 47–56 (1992)

ASTRONOMY AND ASTROPHYSICS

The integrated radio continuum spectrum of M33: evidence for free-free absorption by cool ionized gas

F. P. Israel [1], **M. J. Mahoney** [2,*], **and N. Howarth** [3]

[1] Sterrewacht, Huygens Laboratory, Postbus 9513, NL-2300 RA Leiden, The Netherlands
[2] Clark Lake Radio Observatory, University of Maryland, Borrego Springs, CA, USA
[3] Mullard Radio Astronomy Observatory, Cavendish Laboratory, University of Cambridge, Madingley Road, Cambridge CB3 0HE, UK

Received July 26, 1990; accepted January 21, 1992

Abstract. We present measurements of the integrated radio continuum flux density of M33 at frequencies between 22 and 610 MHz and discuss the radio continuum spectrum of M33 between 22 MHz and 10 GHz. This spectrum has a turnover between 500 and 900 MHz, depending on the steepness of the high frequency radio spectrum of M33 (spectral index $-0.9 > \alpha > -0.7$). Below 500 MHz the spectrum is relatively flat ($\alpha = -0.2$). We discuss possible mechanisms to explain this spectral shape and consider efficient free-free absorption of nonthermal emission by a cool ($T_e \leqq 1000$ K) ionized gas to be a very likely possibility. The surface filling factor of both the nonthermal and the thermal material appears to be small (of order 10^{-3}), which could be explained by magnetic field/density fluctuations in the M33 interstellar medium. We briefly speculate on the possible presence of a nuclear radio source with a steep spectrum.

Key words: galaxies: individual (M33) – galaxies: radio continuum observations – interstellar medium: ionized gas

1. Introduction

Determination of the integrated radio continuum emission over a sufficiently broad range of frequencies supplies valuable information on the global properties of galaxies. For instance, a high-frequency spectral flattening is a signpost of significant thermal emission; accurate determination of low-frequency and high-frequency spectral indices allows separation of the thermal and nonthermal components. Spectral changes at low frequencies may provide additional information on processes such as free-free absorption of nonthermal emission, electron energy losses and on the presence of components such as galactic haloes and steep-spectrum central sources.

Studies of the integrated radio spectrum of galaxies have yielded useful results of this type (e.g. Gioia et al. 1982; Israel & Van der Hulst 1983; Israel & Mahoney 1990). The last authors presented evidence for efficient free-free absorption of the non-thermal emission of spiral galaxies by cool ($T_e < 1500$ K) ionized material. For the nearest galaxies accurate integrated flux-densities are rare at most frequencies. The large extent and low surface brightness of these galaxies, including M31 and M33, makes these determinations difficult. At low frequencies, large observing beams and the steeply rising spectrum of background sources may introduce confusion problems, often leading to an *overestimate* of fluxes. At high frequencies, small observing beams and low surface brightness may make determination of the true baselevel difficult. By underestimating the maximum source extent of a low surface brightness object (especially when the area mapped is not much larger than the source), one places the baselevel too high, thus *underestimating* the high-frequency flux. A small error in the assumed baselevel may easily cause a large error in the integrated flux density. Thus, if observational bias is present, it tends to produce integrated radio spectra that are too steep rather than too shallow.

The Local Group galaxy M33 is of specific interest. It is the nearest late-type spiral; its structure and contents are well-studied. Yet, observations have forced revision of its radio spectral index several times over the last decades as may be illustrated by a brief literature overview. Terzian & Pankonin 1972 estimated a spectral index $\alpha = -0.2 \pm 0.2$ ($S_\nu = \nu^\alpha$) between 318 and 1410 MHz; von Kap-herr et al. 1978 found $\alpha = -0.52 \pm 0.08$ between 318 and 4750 MHz. Over the same frequency range, Beck 1979 found $\alpha = -0.65 \pm 0.03$ and Buczilowski 1988 concluded that $\alpha = -0.91 \pm 0.13$ between 842 and 4750 MHz. This suggests a significant spectral flattening at lower frequencies (cf. Buczilowski 1988). Here, we present an extension of the M33 integrated radio spectrum to the very low frequency of 22 MHz and a discussion of this spectrum over the full frequency range now available.

2. The database

2.1. CLRO observations between 22 and 74 MHz

The new data include measurements at low frequencies obtained in November 1985 with the now defunct Clark Lake Radio Observatory of the University of Maryland, at six frequencies between 16.6 and 73.8 MHz. This telescope consisted of a T-shaped array of 48 linear groupings (banks) of 15 log-spiral

Send offprint requests to: F. P. Israel

* Present Address: Jet Propulsion Laboratory, Mail Stop 168-327, 4800 Oak Grove Drive, Pasadena, CA 91109, USA

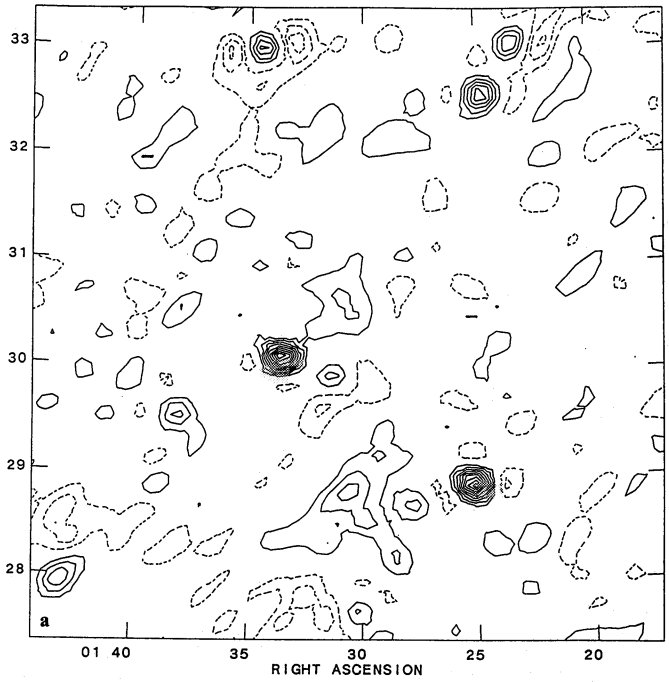

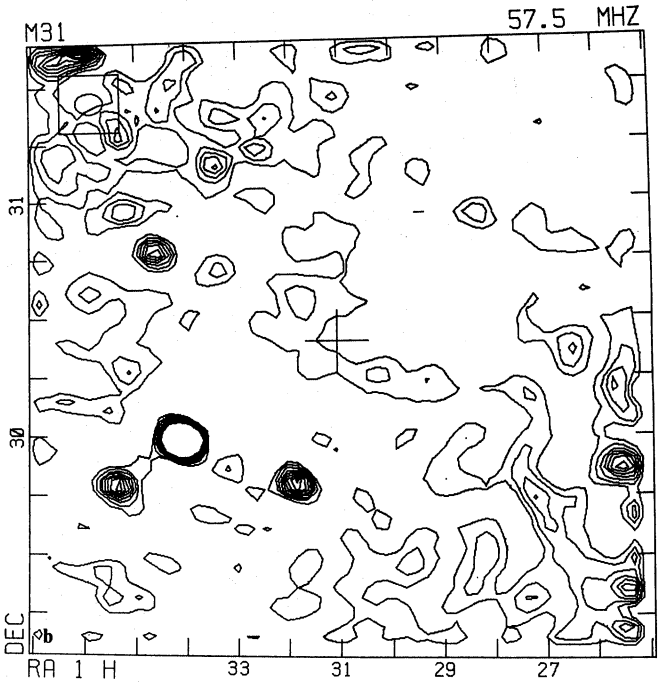

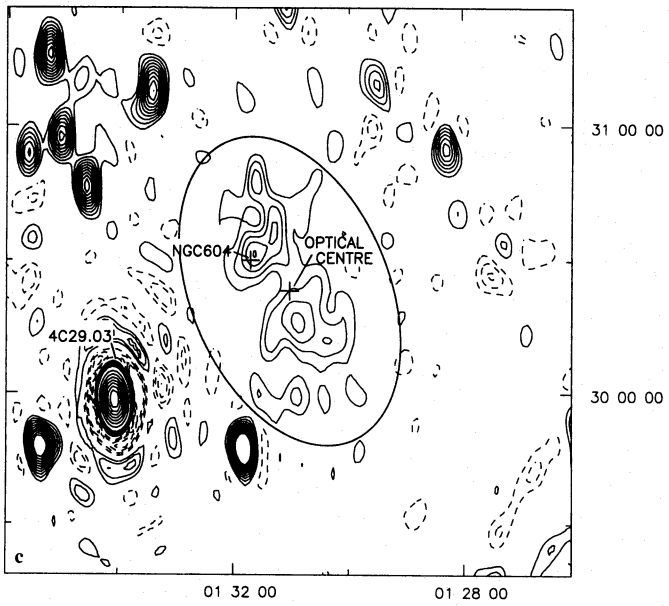

Fig. 1a–d. Maps of the radio continuum emission of M33. Background sources A and I, referred to in the text, are at $\alpha = 01^h29^m24^s.1$, $\delta = +30°28'44''$ and $\alpha = 01^h31^m39^s.9$, $\delta = +30°47'49''$ respectively. **a** CLRO map at 26.5 MHz. Contours are in steps of 4 Jy/beam; zero contour is omitted. 3C48 has been subtracted. **b** CLRO map at 57.5 MHz. Lowest contour is 0.2 Jy/beam; higher contours are in steps of 0.4 Jy beam^{-1}. The baselevel of this map is not corrected for a low spatial-frequency ripple extending from the southwest to the northeast corner. 3C48, outside the map area, was not subtracted. **c** MRAO map at 151.5 MHz. Contour values range from -0.5 to $+0.5$ Jy beam^{-1} in steps of 0.1 mJy beam^{-1}, and from 1 to 11 Jy beam^{-1} is steps of 1 Jy beam^{-1}. The zero contour is omitted. The map is not corrected for primary beam attenuation (approximately 0.94). The ellipse indicates expected maximum radio extent of M33. Within the ellipse, Bonn sources 28 and 9 (I) may be recognized at $\alpha = 01^h31^m$, $\delta = 30°00'$ and $\alpha = 01^h31^m40^s$, $\delta = 30°48'$. **d** WSRT map of M33 at 610 MHz. Gray levels range from 0 to 224 mJy beam^{-1} in steps of 32 mJy beam^{-1}. Contours are in steps of 96 mJy beam^{-1}. Map has been smoothed to a resolution of 3.2×6.8 arcmin. Baselevel was corrected as discussed in Sect. 2.3

elements each. The telescope parameters were optimized for observations around 57.5 MHz. With beamsizes varying from 6 to 15 arcmin, depending on observing frequency, the telescope was well-suited to observations of M33. Further details of the telescope, its mode of operation and reduction procedures are described by Erickson & Fisher (1974) and Erickson et al. (1982). The observations of M33 were reduced and calibrated as described by Israel & Mahoney (1990). The flux density scale used is that of Baars et al. (1977). At 25.6, 30.9 and 57.5 MHz, the galaxy was observed three times on different days. At 22.0 MHz, we obtained two independent observations, while at 16.6 and 73.8 MHz the galaxy was observed only once. As the maps were not limited by theoretical noise, but rather by ionospheric disturbances, confusion and occasional low-level interference, we made no attempt to average them. In Figs. 1a and b we show, as examples, maps at 25.6 and 57.5 MHz. In each map, we determined integrated flux-densities by integrating the signal over different map areas, specifically taking into account baselevel uncertainties and the distribution of recognizable unrelated background sources.

The results are given in Table 1. The results obtained on different days are in good agreement. The single observation at 16.6 MHz was at the limit of the CLRO capability. It yielded no useable result and was not repeated. At 30.9 and 73.8 MHz the galaxy is clearly detected, but a precise value of the actual flux density is difficult to determine, so that we present only upper and

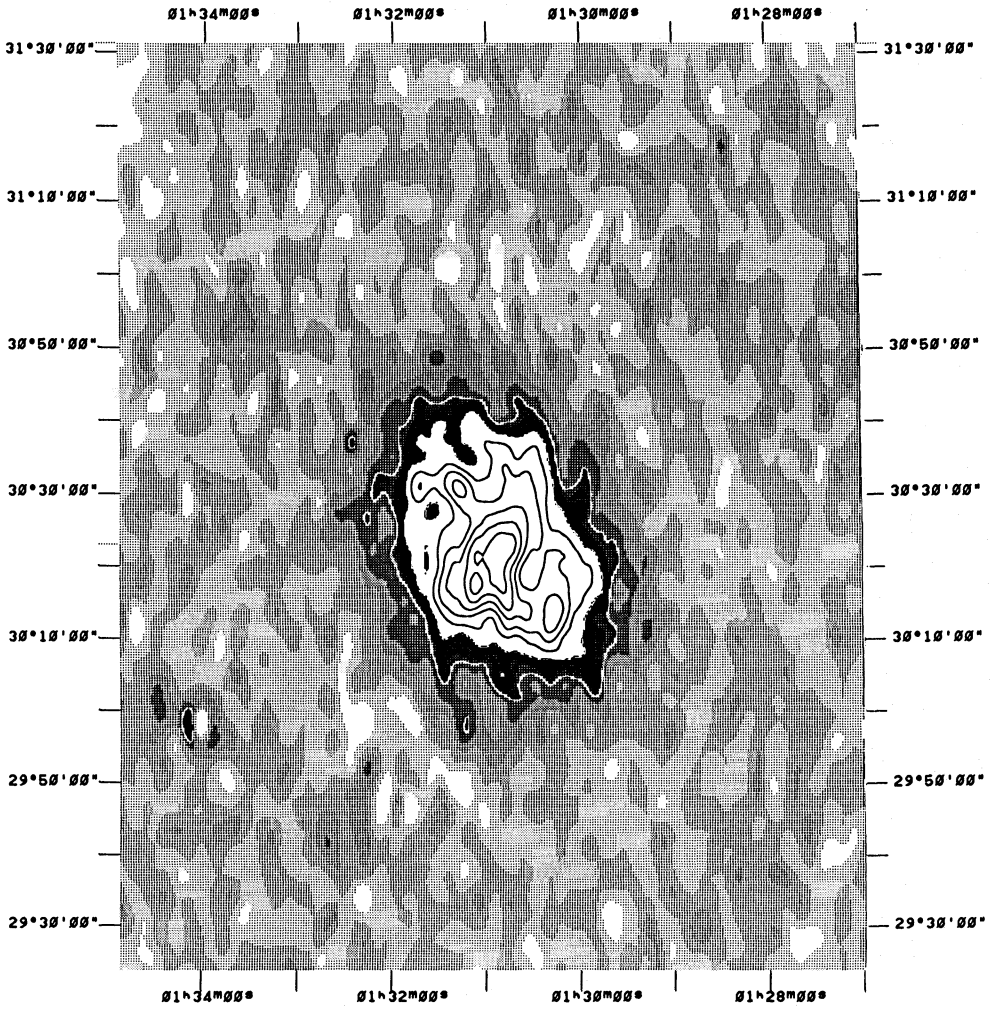

Fig. 1d

lower limits. The major uncertainty in the integrated flux densities is due to (i) the low surface brightness of M 33 combined with the uncertainties in the extent of the emission, and to a lesser extent also to (ii) the relatively high confusion level for a large beam at low frequencies and (iii) uncertainties in the flux scale at these frequencies. The errors given in Table 1 reflect the combined effect of these uncertainties; they are higher than the internal errors suggested by the repeatibility of the measurements. With the uncertainties quoted, a contribution by unrelated background sources is negligible (see Sect. 2.5). As will become clear, all low-frequency flux densities are well below what would be expected from an extrapolation of results obtained at higher frequencies.

Table 1. New flux determinations of M 33

Frequency (MHz)	Beamsize (arcmin)	Flux density[a] (Jy)
21.4	18.2 × 15.6	7 ±3
25.6	15.7 × 13.4	12 ±4
30.9	13.0 × 11.1	6–12
57.5	7.0 × 5.5	7.5 ±2.5
70.4	5.4 × 4.7	3–12
151.5	4.6 × 9.2	5.6 ±1.8
326.4	0.9 × 1.8	5.65±0.8
609.5	0.8 × 1.7	4.4 ±0.6

[a] Flux-density contribution of sources A and I subtracted; see text, Sect. 2.5

2.2. *MRAO observations at 151.5 MHz*

The 151.5 MHz observation was obtained as part of the MRAO Cambridge 151 MHz survey. The telescope provided 776 baselines, ranging from 11.9 to 4600 m in intervals of 5.9 m. Only the 200 shortest baselines out to 1200 m were used, resulting in a synthesized beam of 4.6 × 9.2 arcmin. The primary beam has a FWHM size of 17°, and the first grating ring is at 18°. Structure on scales larger than 5° is not represented. Several observations were available, as M 33 is included in the 3C 48 calibrator field. Of these, eight were selected for inclusion, representing data taken between 1984 and 1988. In the reduction stage, 3C 48 was removed from the field after application of a first order ionospheric correction. The map zerolevel was determined by blanking off the region around every source with a flux density of 4σ (rms) in a region of 4.3 × 4.3 degrees. The map noise level (1σ) is about 100 mJy beam^{-1}, the nominal zero level was found to be at -30 ± 10 mJy beam^{-1}. The integrated flux density of M 33 was found by integrating the map over a varying area. Here we have

assumed 3C 48 to have $S_{151} = 64$ Jy (Laing & Peacock 1980); the consistency of the flux calibration was verified on 4C+29.03 which in the map has $S_{151} = 9.8 \pm 0.2$ Jy, in perfect agreement with the spectrum given by Buczilowski & Beck (1987). The error in the integrated flux-density of M 33 is about 30%, mostly caused by the map zerolevel uncertainty (22%) and the map noise (17%).

The 151.5 MHz map is shown in Fig. 1c. It is at least qualitatively similar to the map at 610 MHz (Fig. 1d). The southern spiral arm of M 33 can be recognized, as well as the giant H II region complex NGC 604 and background source I, which contributes about 0.2 Jy (cf. Sect. 2.5). At the position of Bonn source 28 a feature is seen in the map; however this source has $\alpha(610\text{–}4750) = -0.85 \pm 0.15$, so that only $S_{151} = 55 \pm 15$ mJy may be due to this object. Background source A was subtracted from the map before the integration and therefore does not contribute. The integrated 151.5 MHz flux density is slightly below the CLRO values at lower frequencies.

2.3. *WSRT observations at 327 and 610 MHz*

Integrated flux densities at 327 MHz and 610 MHz were obtained from maps made with the Westerbork Synthesis Radio Telescope. The observations, their reduction and calibration ware described elsewhere (Deul et al. in preparation; Israel in preparation). The 610 MHz map is shown in Fig. 1d. In both maps, the negative baselevel was corrected to true zero by using the procedure outlined by Braun & Walterbos (1985).

That method also restores most of the flux that might be missing due to the lack of spacings shorter than 36 m. This effect would be most serious for the 610 MHz observation. At this frequency a *uniform source at* $\delta = 90°$ of dimensions 10 arcmin would suffer 15% dilution at a 36 m spacing. If, for such a source, the diameter were 30 arcmin, dilution would be 75%. Because M 33 is at $\delta = 30°.5$, dilution in the declination direction is much less; this is fortunate, as the galaxy has its largest extent in declination. Moreover, as the restoration method used in effect extrapolates fringe visibilities to zero spacing, it corrects the dilution for in principle all emission out to about 3/4ths of the first grating ring radius (which is 93 × 183 arcmin in the 610 MHz map used). Integrated flux densities were determined by summing map intensities over increasing areas up to $\alpha \times \delta = 85 \times 165$ arcmin, after removal of the strongest background sources (including sources A and I – see Sect. 2.5), and by extrapolating the background to its "zero pixel value". Virtually all of the emission from M 33 is contained in a box of dimensions $\alpha \times \delta = 45 \times 85$ arcmin.

The 327 MHz date were treated in a similar manner. Here, dilution of extended emission in the original map is a less important problem. To first order, the procedure used removes the contribution by the remaining background sources from the integrated flux density of M 33. If our flux restoration method was only partially successful, in particular the flux density at 610 MHz listed in Table 1 could be somewhat underestimated. The 610 – 327 MHz spectrum would be flatter since necessarily more flux would have been missed at 610 than at 327 MHz. Comparison of the 327 and 610 MHz maps provides, however, no indication that this should be the case.

2.4. *Radio data from the literature*

In Table 2 we have listed observational results at other frequencies. Where necessary, we reduced the values listed to the flux

Table 2. Previously published integrated flux determinations of M 33[a]

Frequency (MHz)	Beamsize (arcmin)	Flux density (Jy)	Reference
178	14 × 276	10 ±4[b]	Leslie (1960)
318	17	7.7 ±1.2	Terzian & Pankonin (1972)
408	3 × 10	6.0 ±0.6	Braccesi et al. (1967)
606	10	6.0 ±0.6	Terzian & Pankonin (1972)
750	18.5	6.6 ±1.8	Venugopal (1963)
750	18.8	4.8 ±2.5[d]	De Jong (1965)
842	15	5.4 ±1.2	Buczilowski (1988)
1400	10	4.1 ±1.5[c]	Venugopal (1963)
1410	10.0	3.2 ±1.7[d]	de Jong (1965)
1410	10.4	3.2 ±0.5[d]	Dennison et al. (1975)
1415	4 × 24	4.3 ±0.4	Huchtmeier (1975)
1420	9.2	3.0 ±0.4	Buczilowski (1988)
1720	7.7	2.7 ±0.25	Buczilowski (1988)
2695	5.2	2.4 ±1.0[d]	Dennison et al. (1975)
2702	4.4	1.7 ±0.17	Buczilowski (1988)
4750	2.4	1.1 ±0.17	Buczilowski (1988)
4850	2.4	1.4 ±0.3	von Kap-herr et al. (1978)
10700	1.2	0.55 ±0.15[e]	Buczilowski (1988)

[a] Flux density contribution by sources A and I subtracted
[b] Flux scale unknown
[c] Redetermined by planimetering published map and assuming 4C+29.03 to have $S_{750} = 2.45$ Jy and $S_{1400} = 1.40$ Jy (cf. Buczilowski & Beck 1987)
[d] Rescaled to flux scale of Baars et al. 1977
[e] Considered to be a lower limit; see text

density scale given by Baars et al. (1977). All values are corrected for the contribution by background sources A and I. This correction is, in any case, small at all frequencies (Sect. 2.5).

Virtually all previously published flux densities below 1000 MHz are considerably *above* our WSRT points. As discussed in Sect. 2.3, we do not believe that we have underestimated these flux densities by a significant amount. The very old 178 MHz value (Leslie 1960) has a large uncertainty; the flux scale is not mentioned, and the observation is probably confused with 3C 48 as the observing beam was very extended in declination. We will therefore ignore this determination. The relatively old maps published by Terzian & Pankonin (1972) at 318 and 606 MHz show that their flux densities, especially at 318 MHz, are critically dependent on the assumed baselevel. A shift upwards of 1.4 K (which corresponds to about half of the lowest contour value in their map) is sufficient to bring the 318 MHz flux density into perfect agreement with our 327 MHz value. The observations by Venugopal (1963) lack an indication of the flux scale used. We have planimetered the published maps, and determined the flux scale by determining the flux densities of 4C+29.03 from the spectrum given by Buczilowski & Beck (1967). The resulting values, although with a large uncertainty, are significantly below the values published. We conclude that none of the older measurements of M 33 forces us to revise our WSRT values.

The 610 MHz point is still lower than would be expected from the Bonn 842 MHz point (Buczilowski 1988). That point fits the steep spectrum derived from his higher frequency observations. Since flux densities in the 1–2 GHz range appear to be well-established, the steepness of this spectrum depends on the flux at 4.75 GHz. The total flux-density of M 33 at 10.7 GHz was derived from a limited map at this frequency by using the 4.75 GHz radial profile and the spectral index as a guideline. Thus, the 10.7 GHz flux is not independent from the 4.75 GHz result and carries no substantial weight in the determination of the M 33 spectrum (Buczilowski 1988).

2.5. Background sources

Here, we discuss the need to apply corrections for unrelated background sources possibly contaminating M 33 flux densities. Background sources have been measured at various frequencies by Israel & Van der Kruit 1974, Viallefond et al. 1986, Buczilowski & Beck 1987, Israel in prepraration and Deul et al. in preparation. The potential importance of background sources may be illustrated as follows. In the 610 MHz map, we found distributed over the face of M 33 a total of 19 sources with $S_{610} > 10$ mJy which appear unrelated to the galaxy. Half of these have flux densities below 20 mJy and have not been identified in the Bonn maps (Buczilowski & Beck 1987). The sum flux of these 19 sources is $S_{610} = 645$ mJy; if they would all have a spectral index $\alpha = -0.8$, they would contribute significant flux densities of 1.1, 2.0, 4.3 and 8.2 Jy at the respective frequencies of 327, 151, 57.5 and 25.6 MHz. Note that sources A and I (cf. Israel & Van der Kruit 1974) contribute 37% to these totals. Several factors, however, alleviate this potentially serious contamination of M 33 flux densities. First, all flux densities were derived by subtracting a base level determined in the vicinity of the galaxy. Since the weaker sources are more or less uniformly distributed over the sky, their contribution to the M 33 flux density will thus be cancelled to first order. The relatively strong source A (Source 3 in the nomenclature of the Bonn observers) with $S_{610} = 140$ mJy has a spectral turnover at about 1 GHz, as indicated by its flux density $S_{327} = 80$ mJy (Deul et al. in preparation). Source I (S9 in Bonn nomenclature) has a relatively flat spectrum with $\alpha = -0.6$ (Buczilowski & Beck 1987). Although these two objects are not dominant contributors to the emission at low frequencies, we have subtracted their contribution from the values in Table 1 to avoid any problems.

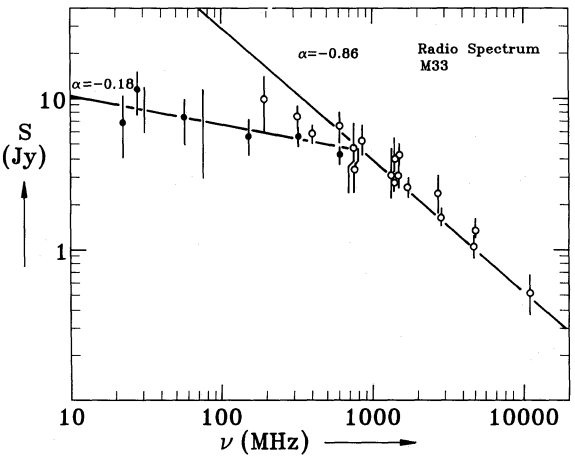

Fig. 2. Radio continuum spectrum of the integrated emission from M 33. Filled circles and bars without circles are new data from Table 1, open circles are literature data from Table 2. Model spectrum fitted is solution 1 from Table 3

The strongest field source is 4C+29.03 (Bonn source 17), with $S_{610} = 2.7$ Jy and $\alpha = -0.87$. At a distance of 47 arcmin to the M 33 nucleus it does not directly influence our measurements of the galaxy. Likewise, Bonn sources 19 and 20 are located at large distances of 46 and 70 arcmin to the nucleus of M 33 and are not a problem at any frequency. These sources were removed from the WSRT maps before the map intensity sums were determined and therefore do not influence the baselevel either. Thus, with the exception of sources A and I, the data indicate no need to apply significant corrections for unrelated sources to the integrated flux densities in Table 1, as is e.g. confirmed by the 151.5 MHz map in Fig. 2. We have verified this further on the 610 MHz map. Our extrapolation to "zero-pixel sum" suggests an integrated background flux of 450 mJy over the face of M 33; when we add to this a contribution of 230 mJy due the subtracted sources A and I, the total background correction at 610 MHz becomes 680 mJy, as compared to the observed sum flux of 645 mJy due to suspected background sources stronger than 10 mJy.

3. Analysis

3.1. The observed M 33 radio spectrum

In Fig. 2 we show all available radio continuum data on M 33. Our new observations are indicated by filled circles and (revised) literature values are shown as open circles. Vertical bars represent quoted errors. The two low-frequency points of poor reliability are indicated by vertical bars only. We have analysed the M 33 radio spectrum in terms of two power law spectra at low and high frequencies respectively. In this analysis, we used only the 22–610 MHz data presented in this paper (with the exception of the 30.9 and 73.8 MHz results) and the 842–4750 MHz data from Buczilowski (1988) as we considered that inclusion of the remaining literature data would not contribute to the overall accuracy of the results. We also investigated the influence of the assumed break frequency and of individual fluxes on the result. Represen-

Table 3. Power law decomposition of M33 radio spectrum[a]

Solution	Break frequency (MHz)	α (low)	α (high)	$\Delta\alpha$	Excluded frequency points (MHz)
1	875	−0.17	−0.86	+0.69	None
2	845	−0.18	−0.86	+0.68	610, 842
3	610	−0.20	−0.69	+0.49	842
4	555	−0.17	−0.61	+0.44	842, 4750
5	910	−0.17	−0.91	+0.74	4750

[a] See text, Sect. 3.1

tative cases are given in Table 3 and shown in Fig. 3. The low-frequency spectral index is rather insensitive to inclusion or exclusion of specific frequency points (hence on break frequency) up to 1420 MHz: $\alpha = -0.18 \pm 0.04$. The results for the high frequency spectral index are somewhat less certain. Assigning equal weight to all points, we find a break frequency of 875 ± 75 MHz and a high-frequency spectral index $\alpha = -0.86 \pm 0.05$. Exclusion of the 610 and 842 MHz points yields the same result. In both cases we find a spectral break magnitude $\Delta\alpha = 0.7 \pm 0.06$. Similar results are obtained by excluding various combinations of the 610, 842 and 4750 MHz points. A different result may be obtained by assuming that the 842 MHz point is unleliable and that the 610 MHz point refers to the high-frequency radio spectrum of M33. The break frequency is then forced to 600 ± 50 MHz and $\Delta\alpha = 0.5 \pm 0.06$. If we were to give the 4750 MHz point lower weight, we may even obtain a break frequency of 555 ± 50 MHz with $\Delta\alpha = 0.45 \pm 0.07$. Here we stress that all solutions, except the last one, are consistent with the observed fluxes within the quoted errors and that the linear regression fits on the high-frequency data points have for all solutions similar correlation coefficients typically $n \approx 0.97$.

Thus, if we take the fluxes given by Buczilowski (1988) at face value, the data clearly suggest a spectral break $\Delta\alpha = 0.7$ at about 850 MHz and a high-frequency spectral index $\alpha = 0.86$. A lower break frequency and a lesser break magnitude $\Delta\alpha = 0.5$ can only be obtained if the 842 MHz integrated flux density of M33 is lower than stated and if the high-frequency spectral index is $\alpha = -0.7$. An even less steep high-frequency spectrum with $\alpha = -0.6$ provides a relatively poor fit to the data and requires a 4750 MHz flux about 20% higher than given by Buczilowski (1988). Whatever the case, a turnover must be present in the M33 radio spectrum in the 500–900 MHz range. In extended, low surface-brightness radio sources as M33 such a turnover may be caused by energy losses of relativistic electrons or by free-free absorption. We will consider these possibilities in turn.

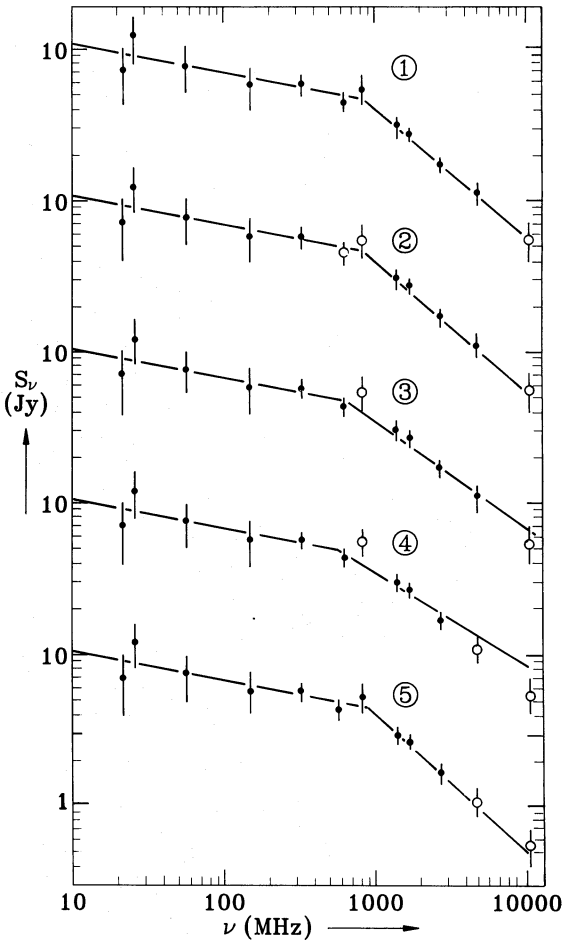

Fig. 3. Various fits to data from Table 1 and Buczilowski (1988), as discussed in the text, Sect. 3. The spectra are numbered according to the solutions in Table 3

3.2. *Nonthermal energy losses*

A spectral turnover $\Delta\alpha = 0.5$ at a frequency ν_t GHz implies a residence time t years for the relativistic electron population given by $t^2 = 0.3\, B^{-3}\, \nu_t$ where B is the magnetic field strength in gauss. If $\Delta\alpha > 0.5$, the steady-state models do not apply, unless two or more electron energy loss mechanisms have turnover frequencies sufficiently close that a combined $\Delta\alpha > 0.5$ results. Such a situation is in fact proposed by Pohl et al. (1992) for the galaxy NGC 4631. However, crucial elements in their solution are the existence of a massive dark halo, not directly observed, fed by a postulated cooling flow. A priori, this interpretation cannot be ruled out, but we point out that it remains a hypothesis until independent observations confirming the underlying assumptions have become available.

If a non-steady state model is assumed, the magnitude and frequency of the spectral turnover indicate instead a drop of the relativistic injection rate t years ago. Such a situation appears to be found in the small dwarf irregular galaxy NGC 1569 (Israel & De Bruyn 1988). With $\nu_t = 0.85$ GHz and $\Delta\alpha = -0.7$, M33 could be an analogue to the much smaller NGC 1569: relativistic electron

injection rates would have sharply dropped only 65 ± 25 million years ago for magnetic field strengths of 4 ± 1 μG (Buczilowski & Beck 1991). Unlike NGC 1569, M 33 shows no trace of the energetic events that must have preceded this drop. Moreover, Israel & De Bruyn (1988) have argued that injection rate variations are unlikely to dominate the radio emission from galaxies such as M 33, which is much larger and more massive than NGC 1569.

The lowest break frequency consistent with the data is $\nu_t = 0.6$ GHz with $\Delta\alpha = 0.5 \pm 0.05$; in that case steady-state models clearly could apply with a characteristic residence time of relativistic electrons $t = 55 \pm 25$ million years for a magnetic field strength of 4 ± 1 μG. If magnetic field strengths are higher, due to magnetic field clumping, this residence time would be even shorter (as indeed also the time elapsed since injection rates decreased in the previous case). If M 33 suffers from significant high-energy electron losses, the current relativistic electron injection spectrum must be reflected by the low-frequency radio spectral index. Its value $\alpha = -0.18 \pm 0.04$ implies a current injection spectrum $dE = \text{cst}\, E^{-\gamma}$ with $\gamma = 1.36 \pm 0.08$. It is hard to identify the source(s) of such a flat injection spectrum in M 33. This objection would, however, be alleviated if ionization losses could be shown to be important at the low frequencies observed.

Yet another possibility is a break in the nonthermal spectrum introduced by the presence of galactic winds in M 33. Winds perpendicular to galactic planes have been proposed by e.g. Lerche & Schlickeiser (1982). Although solid evidence for wind occurrence is still lacking, their model calculations indicate that a spectral break of magnitude $\Delta\alpha = 0.5$ will occur at a frequency below 1 GHz in adiabatic cooling haloes; no such break occurs in static or pure convection haloes. Possibilities and problems of this interpretation for various galaxies are discussed in a recent paper by Pohl et al. (1991). For M 33, a break frequency of 850 MHz in a homogeneous magnetic field of 4 μG implies a wind of $V_\infty = 35\ \text{km s}^{-1}$ and an adiabatic cooling time of 85 million years. However, a spectral index change $\Delta\alpha = 0.7$ appears to be well in excess of the predicted break magnitude $\Delta\alpha = 0.5$. Only for high-frequency spectral indices $\alpha \leqq 0.7$ would the break magnitude reduce to the required magnitude. Moreover, the asymptotic low-frequency spectral index should approach a value corresponding to the relativistic electron injection spectral index. As shown above, the observed low-frequency spectrum appears to be too flat.

Moreover, the observed spectral index change is, in fact, a lower limit to the actual change in the nonthermal spectrum. At higher frequencies flat-spectrum thermal emission contributes increasingly significant amounts to the emission, flattening the GHz spectrum, but hardly influencing the low-frequency spectrum. Buczilowski (1988) estimates an intrinsic nonthermal spectral index $\alpha = -1.1$ for an observed high-frequency spectral index $\alpha = -0.9$, so that $\Delta\alpha\,(\text{nonthermal}) = 0.9$. In a flatter high-frequency spectrum, the thermal fraction will be higher, again yielding a nonthermal spectral break well in excess of $\Delta\alpha = 0.5$.

In a clumped magnetic field, the resulting higher magnetic field strengths would modify the above estimates. For instance, a ten times stronger field (40 μG) will decrease characteristic residence and adiabatic cooling times by a factor of 30, and increase the wind velocity likewise to about $1000\ \text{km s}^{-1}$. Yet, such an increase would not raise the spectral turnover due to ionization losses sufficiently close to the observed M 33 turnover frequency to explain a spectral break of a magnitude in excess of 0.5. Whether even stronger magnetic fields exist in a highly clumped, but low-density medium is questionable. Moreover, we would expect that a strong, large-scale wind would tend to smoothen inhomogeneities rather than enhance them.

We conclude that simple steady-state models of relativistic electron energy losses are incompatible with the observed M 33 spectrum, and we consider more complex models involving cooling flows or galactic winds unattractive in this particular context. Instead, we prefer to interpret the observed M 33 spectrum in terms of free-free absorption. As is clear from the following (and I&M) this presupposes the existence of significant amounts of low-temperature (partly) ionized gas. The existence of such a gas is generally predicted by time-dependent models of the interstellar medium (see Gerola et al. 1974; also Bania & Lyon 1980).

3.3. *Free-free absorption*

From a comparison of observed 57.5 MHz flux densities with extrapolated radio continuum spectra of several spiral galaxies, Isarael & Mahoney 1990 (hereafter I&M) gave evidence for free-free absorption of nonthermal emission by a cool ($T_e \leqq 1500$ K) tenuous gas; high absorption efficiencies suggest a strong spatial correlation between thermal and nonthermal material (but see also the criticism by Hummel, 1991). If this situation applies to M 33, its better sampled low-frequency spectrum yields additional constraints on model input parameters. We first consider the simple model described by I&M. Nonthermal emission arises in a homogeneous cylindrical volume; absorption takes place in an embedded homogeneous cylinder which scales by a factor a ($0 \leqq a \leqq 1$) with the nonthermal cylinder. From I&M:

$$S_\nu / S_{\nu,0} = 1 - a^2 + 1/2\, a^2 (1-a)\,(1 + e^{-\tau_\nu}) + a^3 [(1 - e^{-\tau_\nu})/\tau_\nu] \quad (1)$$

Here S_ν is the observed flux density at frequency ν, and $S_{\nu,0}$ is the (extrapolated) nonthermal flux density in the absence of free-free absorption. If the scaling parameter $a < 1$, for very large optical depths τ_ν (i.e. at very low frequencies) the unabsorbed fraction of the nonthermal emission will have the same spectral index as the nonthermal emission at frequencies for which $\tau_\nu \ll 1$. At such low frequencies, observable flux densities S_ν asymptotically approach:

$$S_\nu / S_{\nu,0} = 1 - 1/2\, a^2 - 1/2\, a^3 . \quad (2)$$

In Fig. 4, we give the predicted radio spectrum for several values of the scaling parameter a normalized to $S/S_0 = 0.54$ (for $\alpha\,(\text{high}) = -0.86$) and 0.75 (for $\alpha\,(\text{high}) = -0.69$) at 327 MHz and calculated following Eq. (1). The best values are $a = 0.95 \pm 0.03$, and $a = 0.91 \pm 0.02$ respectively. This is in good agreement with the conclusion reached by I&M for other spiral galaxies that a large fraction of the nonthermal emitting volume is filled with absorbing thermal material. At 327 MHz the corresponding model optical depths are $\tau = 1.7 \pm 0.3$ and 0.8 ± 0.1. Somewhat lower values may be obtained by assuming the nonthermal emissivity to increase towards the galactic plane with respect to the absorbing plasma. Correction for the assumption $\alpha\,(\text{NT}) = \alpha\,(\text{high})$ results in only slightly higher values for a. Likewise, minor changes in the normalization hardly change the result. Model optical depths *do not change* if nonthermal emissivity and thermal absorptivity vary along the line of sight in constant proportion. Therefore, this result is also valid for e.g. a clumped distribution.

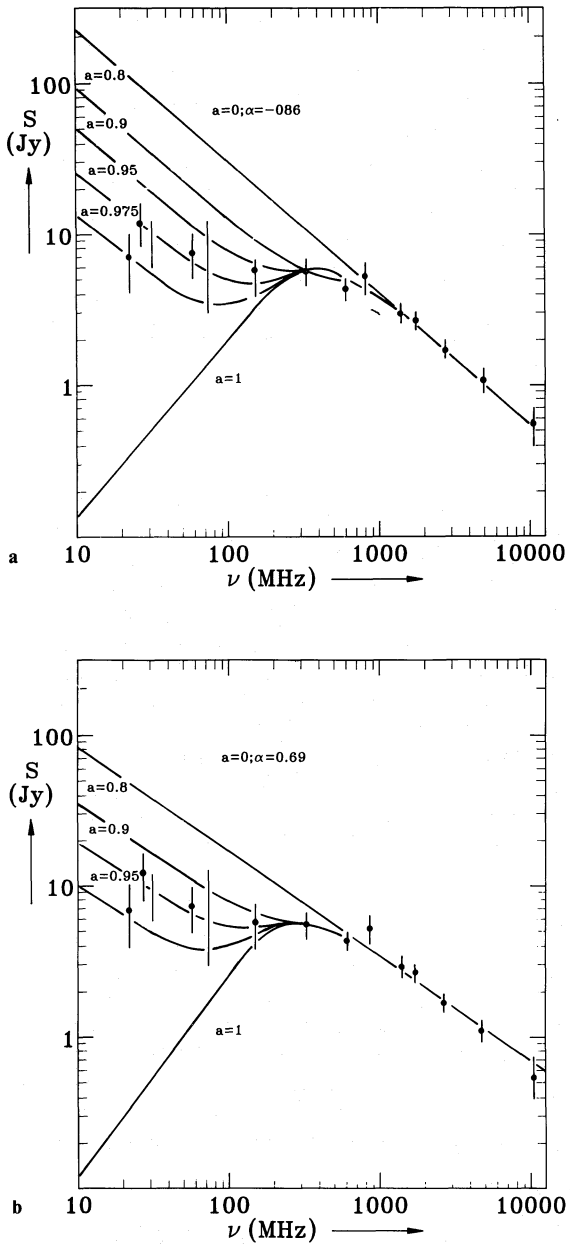

Fig. 4a and b. Model radio continuum spectra, assuming free-free absorption, compared with integrated flux densities below 1000 MHz. Several spectra, corresponding to different values of the scaling parameter a (see text) are given. **a** High-frequency spectral index $\alpha = -0.86$ (solution 1 in Table 3). **b** As **a**, but with $\alpha = -0.69$ (solution 3 in Table 3)

4. Discussion

4.1. *Clumpiness of the cool ISM in M33*

A clumpy distribution of both emitting nonthermal and absorbing thermal material is more likely than a homogeneous distribution (cf. I&M). Clumpy distributions also relax otherwise stringent upper limits on possible electron temperatures. Following the general approach by I & M, we find temperatures of a few hundred K for the most reasonable assumptions for the amount of ionizing power P_{44}, line-of-sight r_{NT} and mean electron density $\langle n_e^2 \rangle^{1/2}$. For instance, if $\langle n_e^2 \rangle^{1/2} = 0.10\,\mathrm{cm}^{-3}$, $P_{ion} = 1.0\ 10^{42}\,\mathrm{erg\,s}^{-1}$ (i.e. about half the value assumed for the Galaxy) and $r_{NT} = 3000$ pc (taking into accound the tilt of M33), we obtain $T_e = 250$ K with a surface clumping factor of $5\ 10^{-4}$. Lower values $\langle n_e^2 \rangle^{1/2} = 0.05\,\mathrm{cm}^{-3}$ together with a higher $P_{ion} = 2\ 10^{42}\,\mathrm{erg\,s}^{-1}$ lead to lower electron temperatures $T_e = 50$–100 K and surface clumping factors f_c^2 up to $5\ 10^{-3}$. Only for the somewhat extreme values $P_{ion} = 0.2\ 10^{42}\,\mathrm{erg\,s}^{-1}$ and $r_{NT} = 6000$ pc do we obtain $T_e = 1000$ K, with a very small surface clumping factor of $4\ 10^{-5}$. Note that a temperature $T_e \leqq 250$ K is not unlikely for e.g. a partially ionized cold medium.

We now consider low-frequency free-free absorption in M33 in more detail. The corresponding strength of the thermal radio emission at higher frequencies such as 5 GHz is (I&M):

$$S_5\,\vartheta^{-2} = 4.74\,T_e^{1.15}\,\nu^2\,\tau_\nu\,[\ln(4.96\ 10^{-2}\,\nu^{-1}) + 1.5\ln T_e)^{-1} \quad (3)$$

in which S_5 is the optically thin emission at 5 GHz in mJy, due to the absorbing gas, ϑ^2 is the effective (cylindrical) thermal surface area, T_e is the electron temperature in K, and τ_ν is the absorption optical depth at frequency ν. For a typical temperature $T_e = 250$ K and $\tau_{327} = 1.5$, the surface brightness of the effective emitting area must be about $S_5\,\vartheta^{-2} = 120$ mJy arcmin^{-2}. The *observed extended distribution of radio emission* rules out any significant role by the visual H II regions (which have $T_e = 10^4$ K): they cover much too small a fraction of the nonthermal disk to account for the free-free absorption implied by Fig. 4. The *effective* radio size of M33 is of order 1000–1700 square arcmin (Sect. 2.3). Thus, taking the above surface clumping factors, the 5 GHz emission due to low-frequency absorbing gas alone in M33 is then of order 60 mJy, or about 5% of the total 5 GHz emission of the galaxy, which is mall compared to the thermal flux at 5 GHz contributed by hot H II regions.

Observations of the diffuse Hα emission in M33 indicate an average emission measure at $R = 1$ kpc (corresponding to 5′ on the sky) EM = 79 pc cm^{-6} if $T_e = 10^4$ K (Torres-Peimbert et al. 1974). The quantity $T_e^{-0.81}$ EM is approximately constant over the range $10^2\,\mathrm{K} < T_e < 10^4$ K (cf. Martin 1988) and has the observed value $4.6\ 10^{-2}$. For $T_e = 250$ K, we find $T_3^{-0.81}\,\mathrm{EM} = 1.0\ 10^{-2}$. (For comparison: the results by Torres-Peimbert et al. (1974) imply $T_e^{-0.81}\,\mathrm{EM} = 5\ 10^{-3}$ for the Galactic disk at the position of the Sun.) Thus, in M33 about 20% of the observed diffuse Hα emission should be due to low electron temperature ionized gas. The clump density at $T_e = 250$ K is of order 5 cm^{-3}. If the clumps are in pressure equilibrium with a homogeneous interclump gas, this should have a density of 0.13 cm^{-3} at $T_e = 10^4$ K. The emission measure of this interclump gas should be EM = 55 pc cm^{-6}. The total quantity $T_e^{-0.81}\,\mathrm{EM} = 4.2\ 10^{-2}$ is then in very good agreement with the observed value.

A surface clumping factor of order 10^{-3} as derived above is quite small even when we take into account the observed structure of M33 (radio emission concentrated towards the center, spiral arm enhancement and extended zones between the spiral arms apparently void of material; Deul & Den Hartog 1990). We believe that it can be explained as follows. Nonthermal emissivity is proportional to the square of the magnetic field strength, while thermal absorptivity is proportional to the square of the electron density. Hence, in compression regions *both* increase in the same way. This suggests that the flattening of the low-frequency radio spectrum of M33 preferentially originates in those parts of the disk which are density-enhanced. Taking a surface filling factor of 10^{-3} for the emitting/absorbing material and considering the relatively smooth radio appearance of M33 in beams of about

30 arcsec, we estimate that significant structure in the disk/spiral arm emission should be present on scales of a parsec, which is not unreasonable. As the necessary degree of clumping of the magnetic field depends very strongly on precisely how the spatial distribution of thermal electrons correlates with that of the magnetic field, it is very difficult to say anything with certainty about it.

A final remark is in order. If higher temperatures of order $T_e = 10^3$ K or more apply (closer to the regime of the Warm ISM as discussed by e.g. Kulkarni & Heiles 1987), we require clumping factors smaller by an order of magnitude or more. In that case, pressure equilibrium could only exist for interclump electron temperatures T_e of order 10^5 K or higher.

4.2. A steep-spectrum source in the nucleus of M33?

Although the above gives a satisfactory explanation for the observed radio continuum spectrum of M33, we wish to speculate briefly on the possibility that the apparent flatness of the spectrum at the lowest frequencies reflects the presence of an additional radio component not seen at higher frequencies. This in effect presumes the scaling parameter a to be unity. In that case the disk flux steadily drops with decreasing frequency: for large values of τ, $(1-e^{-\tau})/\tau$ reduces to $1/\tau$, causing a change in spectral index $\Delta\alpha = 2$ (Fig. 4). Pushing the $a = 1$ curve upwards as far as compatible with the observational error bars, we have a significant flux density excess only below 75 MHz. This could then indicate an additional nonthermal component with a spectrum constrained by its non-detection at 327 MHz ($S_{327} \leqq 20$ mJy), yielding very roughly $S_{20-25} \approx 10$ Jy and $\alpha \leqq -2.3$.

This speculation is not entirely ad-hoc as both the Galaxy and M31 appear to contain such steep-spectrum nuclear sources. At the distance of M33, the Galactic Centre source would have a flux density $S_{110} = 10$ mJy and $\alpha \leqq -1.0$ (Larosa & Kassim 1985; Kassim et al. 1986), much less than the 2 Jy or so implied by $S_{25.6} = 5.5$ Jy, $\alpha \leqq -0.6$ for the source in the nucleus of M31 (Cane & Erickson 1986). Thus, M33 could just barely possess a nuclear source comparable to the one in M31, albeit with a much steeper spectrum. Although the nature of steep-spectrum nuclear sources is unclear, we note that the X-ray luminosity of the M33 nucleus is 10^3 times that of the Galactic Centre and comparable to the X-ray luminosity of the M31 bulge population (Trinchieri et al. 1988; Watson et al. 1981; Van Speybroeck et al. 1979). If such a source were present in M33, it would not change much in our conclusions. The turnover of the spectrum at 500–900 MHz would remain and the break magnitude would increase, if anything.

5. Conclusions

New determinations of the integrated radio continuum flux density between 20 and 327 MHz show that the radio spectrum of M33 becomes noticeably flatter below 1 GHz. Although we cannot completely rule out a spectral break resulting from large-scale galactic winds or other mechanisms causing relativistic electron energy losses, we prefer to interpret the result as caused by free-free absorption by ionized but cool thermal material efficiently filling the nonthermal emitting volume. Electron temperatures are then probably of order 100–250 K. The amount of absorption at low frequencies and the strength of optical H' emission suggest that both the nonthermal and thermal material, although covering most of M33, are strongly clumped (surface filling factor of order 10^{-3}). This can be understood by assuming considerable density fluctuations in the interstellar medium as both nonthermal emissivity and thermal absorptivity increase proportional to the square of the ambient density. The cool ionized clumps could be in pressure equilibrium with a more tenuous and hotter interclump medium without conflict with observational constraints.

The data do not rule out the possibility that M33 contains a steep-spectrum radio source that becomes noticeable only at the lowest observed frequencies. Such a source might occur in the nucleus coincident with the strong X-ray source M33 X-8.

Acknowledgements. It is a pleasure to thank the personnel at the Clark Lake Radio Observatory, the Mullard Radio Astronomy Observatory and the Westerbork Synthesis Radio Telescope for their support. We thank E.R. Deul, U.R. Buczilowski and R. Beck for providing us with material in advance of publication and useful remarks on a previous draft of this paper. Discussions with R.S. le Poole were of great value in clarifying aspects of our analysis, as were several critical remarks by the referee, R. Beck.

References

Baars J.W.M., Genzel R., Pauliny-Toth I.I.K., Witzel A., 1977, A&A 61, 99
Bania T., Lyon J.G., 1980, ApJ 239, 173
Beck R., 1979, Ph.D. Thesis, Univ. Bonn
Berkhuijsen E.M., 1983, A&A 127, 395
Braccesi A., Fanti-Giovannini C., Fanto R., Formiggini L., Vespigniani G., 1967, Nuoveo Cimento B52, 254
Braun R., Walterbos R.A.M., 1985, A&A 143, 307
Buczilowski U.R., 1985, Ph.D. Thesis, Univ. Bonn
Buczilowski U.R., 1988, A&A 205, 29
Buczilowski U.R., Beck R., 1987, A&AS 68, 171
Buczilowski U.R., Beck R., 1991, A&A 241, 47
Cane H.V., Erickson W.C., 1986, in: Low Frequency Radio Astronomy, Erickson W.C., Cane H.V. (eds.). NRAO Workshop No. 10, p. 15
Cruz-Gonzalez C., Recillas-Cruz E., Costero R., Peimbert M., Torres-Peimbert S., 1974, Rev. Mex. Astron. Astrofis. 1, 211
De Jong M.L., 1965, ApJ 142, 1333
Dennison B., Balonek T.J., Terzian Y., Balick B., 1975, PASP 87, 83
Deul E.R., den Hartog R.H., 1990, A&A 229, 362
Erickson W.C., Fisher J.R., 1974, Radio Sci. 9, 387
Erickson W.C., Mahoney M.J., Erb K., 1982, ApJS 50, 403
Gerola H., Kafatos M., McCray R., 1974, ApJ 189, 55
Gioia I.M., Gregorini L., Klein U., 1982, A&A 116, 164
Huchtmeier W.K., 1975, quoted by R.F. Haynes. W.K. Huchtmeier, B.C. Siegmann, A.E. Wright, in: A Compendium of Radio Measurements of Bright Galaxies. CSIRO, Melbourne
Israel F.P., De Bruyn A.G., 1988, A&A 198, 109
Israel, F.P., Van der Hulst J.M., 1983, AJ 88, 1736
Israel F.P., Van der Kruit P.C., 1974, A&A 32, 363
Israel F.P., Mahoney M.J., 1990, ApJ 352, 30 (I&M)
Kassim N.E., LaRosa T.N., Erickson W.C., 1986, Nat 322, 522
Kulkarni S.R., Heiles C., 1987, in: Interstellar Processes, Hollenbach D.J., Thronson H.A. (eds.). Reidel, Dordrecht, p. 87
LaRosa T.N., Kassim N.E., 1985, ApJ 299, L13
Laing R.A., Peacock J.A., 1980, MNRAS 190, 903
Martin P.G., 1988, ApJS 66, 125

Panagia N., Terzian Y., 1984, ApJ 287, 315
Pohl M., Schlickeiser R., Hummel E., 1991, A&A 250, 302
Pohl M., Schlickeiser R., Lesch H., 1992, A&A 252, 493
Terzian Y., Pankonin V., 1972, ApJ 174, 293
Torres-Peimbert S., Lazcano-Araujo A., Peimbert M., 1974, ApJ 191, 401
Trinchieri G., Fabbiano G., Peres G., 1988, ApJ 329, 531
Van Speybroeck L., Epstein A., Forman W., Giacconi R., Jones C., Liller W., Smarr L., 1979, ApJ 234, L45
Venugopal V.R., 1963, PASP 75, 404
Viallefond F., Goss W.M., Van der Hulst J.M., Crane P.C., 1985, A&AS 64, 237
von Kap-herr A., Berkhuijsen E.M., Wielebinski R., 1978, A&A 62, 51
Watson M.G., Willingale R., Grindlay J.E., Hertz P., 1981, ApJ 250, 142